Simultaneous high-speed imaging and laser-induced incandescence (LII) for investigation of the sooting combustion of ethanol fuel blends in a DISI engine

M. Storch[1,2], A. D. Nguyen[1], M. Wensing[1,2], S. Will[1,2], L. Zigan[1,2*]

1) Lehrstuhl für Technische Thermodynamik (LTT), Friedrich-Alexander-Universität Erlangen-Nürnberg (FAU), Erlangen, Germany

2) Erlangen Graduate School in Advanced Optical Technologies (SAOT), FAU Erlangen-Nürnberg

Abstract

In this work the effect of ethanol blending with isooctane on soot formation in a modern optically accessible DISI engine was investigated. An operation point with high sooting tendency comprising piston wetting and poolfire was chosen. Measurements were performed by high-speed combustion imaging of OH-chemiluminescence and natural soot luminosity within the engine together with laser-induced incandescence measurements (LII) in the engine exhaust duct. The results indicate reduced sooting tendency and more homogeneous combustion for blends with high ethanol content (E85 and pure ethanol). The lower soot concentrations can be attributed to different chemical soot formation mechanism in ethanol flames. In addition, indications were found that the mixture formation process is different for ethanol blended fuels in comparison to isooctane.

Introduction

The usage of bioethanol combined with modern innovative engine combustion concepts like direct injection (DI) is beneficial for reaching future CO_2-emission limitations in spark ignition (SI) engine combustion. The drawback of those concepts is the higher particulate matter (PM) emission level [1]. The underlying reason is a reduced fuel and air mixing time, which leads to complex handling of mixture formation processes at engine operation. As a consequence, fuel properties that determine the evaporation and mixing become more significant.

In general, the sooting tendency of a fuel is determined by physical processes (e.g. atomization, evaporation) and chemical mechanisms (e.g. reaction kinetics, carbon-oxygen ratio). Regarding atomization and mixture formation, the higher liquid fuel density, surface tension and viscosity [2] of ethanol as compared to isooctane, which is used as surrogate fuel, cause larger droplet diameters [3]. In addition, ethanol has a large specific enthalpy of evaporation [2]. This leads to a reduced temperature in the evaporating spray [4]. Together with larger droplet diameters, this property can result in incomplete evaporation and mixture inhomogeneities [5]. Considering the chemical properties, ethanol has a lower carbon-to-oxygen ratio as compared to gasoline and isooctane as a surrogate fuel. This can be advantageous for soot reduction since key intermediate precursor species can be reduced [6]. In addition, McEnally and Pfefferle [7] found out that also the short carbon-chain length of ethanol is beneficial for soot reduction. However, ethanol has a lower heating value as compared to isooctane. For engine combustion, this means that the injected fuel mass has to be increased in order to reach the same engine load. Since the mixing and evaporation time is limited, more liquid fuel mass in the combustion chamber can increase soot formation.

There are several investigations of soot formation and PM emission in DISI engines operated with ethanol-gasoline fuel blends in different research studies. Price et al. [8] and Szybist et al. [9] performed exhaust PM measurements using mobility particle sizers. With increasing ethanol content in gasoline fuel, both studies measured particle emission reductions. In contrast Chen et al. [10] reported increasing PM emissions, which are even higher at cold engine conditions. However, those global PM analysis at special engine geometries and different operating conditions do not allow general predictions about PM emissions. Optical investigations are necessary in order to understand the underlying processes and reasons for different PM emissions.

In a previous investigation [11] various sooting DISI operating points were identified and visualized by high-speed imaging. The study was conducted inside an optical accessible engine with isooctane and variation of ethanol content. With increasing ethanol content, a globally fuel rich mixture showed decreasing soot emissions. Especially for late injection and short mixing times (catalyst heating operation) E20, compared to isooctane, showed unexpectedly high soot radiation levels as well as high concentration of exhaust particles. This behavior may be explained by the high enthalpy of evaporation of ethanol. At short mixing times it was assumed that 20 vol% of ethanol (E20) delays or inhibits the evaporation of the sooting component isooctane.

In this study, the operating points of [11] were taken as basis. In catalyst heating engine operation mode the possibility of piston wetting and poolfire is high. This can be an important source for exhaust particulate emission [12]. For the operating point in this work the se-

* Corresponding author: lars.zigan@cbi.uni-erlangen.de

cond injection was retarded, which causes heavy liquid impingement. Since there are higher injection durations for ethanol blended fuels, the poolfire is expected to be stronger, which may lead to higher soot formation rates. In order to analyze this behavior, simultaneous imaging of OH-chemiluminescence and soot radiation was conducted together with laser-induced incandescence (LII) engine exhaust particle concentration measurements. This combined approach allows statements about premixed and sooting combustion as well as soot oxidation processes.

Experimental Setup

The investigations of the present study were performed in a modern single cylinder optical engine based on a series production direct injection engine with lateral injector position. The engine contains two optical accesses, a glass ring liner and an elongated piston with glass window. With this setup, it is possible to illuminate or detect the signal through the glass ring or the piston, respectively, depending on the requirements. In Figure 1 the current setup is displayed. The high-speed camera system images through the glass ring liner, while a broadband 100 W LED array illuminates the injection process (Mie-scattering) through the piston bottom window.

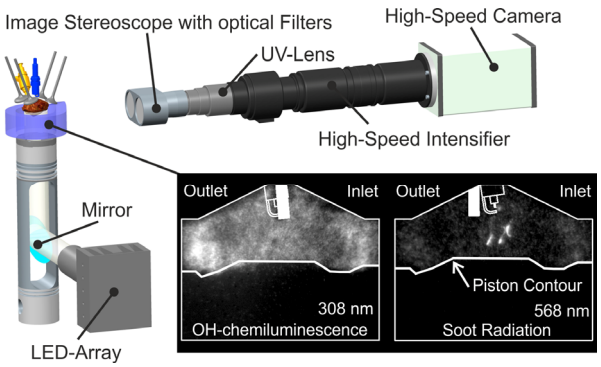

Figure 1. Illustration of the optical imaging setup with glass ring liner and elongated piston. The image on the bottom right shows an example of the combustion process in two different wavelength regions at 46°CA ATDC. The spark plug is marked in the middle of the combustion chamber.

The camera system consists of a Vision Research Phantom v711 high-speed CMOS camera, a novel developed high speed intensifier (Goldlücke Ingenieurleistungen), an UV-enhanced 100 mm (f/2) lens and a LaVision image stereoscope. The camera was driven at a frequency of 7200 Hz which corresponds to 1 image per °CA for 1200 rpm. The images (exposure time: 20µs) were recorded with 1280x648 pixel resolution over 60 cycles, with 100 images per cycle. The image stereoscope contained a set of two different optical filters. The first filter was a 298 nm bandpass filter (FWHM 24 nm, Tmax=29%), which was used to detect the chemiluminescence of the excited combustion species OH, which has its strongest emission peak at around 308 nm [13]. OH* presents a good indicator for flame propagation and heat release rate [14]. The second optical filter was a 568 nm bandpass filter (FWHM 10 nm, Tmax=85%), selected to measure blackbody radiation originating from hot soot particles originated by the flame. An example image of the two wavelength channels can be found in Figure 1. It shows clear separation of sooting combustion and OH-chemiluminescence. The Mie-scattering from the injection event can also be detected through the 568 nm filter. All images were analyzed and processed for each channel separately (background correction, averaging and intensity extraction) by an inhouse code using MATLAB®.

For measuring the exhaust primary particle concentration an inhouse developed laser-induced incandescence (LII) sensor was used in the engine exhaust duct. It is able to measure primary carbon particle concentration in the range of 0.001 to 200 mg/m³ [15].

A typical catalyst heating operating point as it is normally used in cold start operating was analyzed in this work. It is characterized by strong piston impingement and consecutive poolfire, which represents sooting operation. Depending on the fuel, the injection duration is adjusted leading to different piston wetting behavior.

Detailed specifications of this operating point are given in Table 1. The injection pressure was kept constant at 70 bar. Both the engine head and the cylinder liner were conditioned to 70°C, which represents a warm engine. Fuel and air intake temperatures were at 22°C. In addition, the fuels pure isooctane and ethanol as well as the mixtures E20 (20vol% of ethanol in isooctane) and E85 were investigated. The injection duration was adjusted fuel specifically. With this and by keeping the air flow rate constant, a constant air-fuel ratio operation was assured. The spark timing was not adjusted in order to keep the comparability between different fuels regarding soot emissions

Table 1. Specifications of the catalyst heating operating point

Fuel	Isooctane	E20	E85	Ethanol
Engine Speed (rpm)	1200	1200	1200	1200
Air Mass Flow (kg/h)	5.5	5.5	5.5	5.5
λ (-)	1	1	1	1
Engine Load (bar)	2.2	2.4	2.7	2.7
Rail Pressure (bar)	70	70	70	70
SOI1/SOI2 (°CA BTDC)	300/50	300/50	300/52	300/52
Inj. Duration (ms)	0.78/0.48	0.80/0.50	1.08/0.72	1.10/0.73
Spark Timing (°CA BTDC)	0	0	0	0

Results

In Figure 2 an exemplary image series of an injection and combustion event is displayed for isooctane. For this series the two wavelength regions (298 and 568 nm) were matched to one image by image processing.

OH*-chemiluminescence is presented in green and soot radiation in red. Overlapping of these two colors creates "orange" pixel intensities. At the top of the cylinder head, the spark plug is marked in white. Furthermore, the images contain a spark plug cover, in order to prevent overexposure from the ignition event.

At -299°CA and -293°CA ATDC the main injection event can be seen. The images show that already slight piston impingement probably occurs, which does not contribute to higher exhaust emissions since the injection takes place in the intake stroke [11]. Here the fuel has enough time to evaporate completely. Prior to the second injection (-55°CA ATDC), no liquid fuel can be seen in the images. In the cylinder head (close to the spark plug) there is still some "red" scattering signal visible, which is created by reflections from the LED light on metal surfaces. At -49°CA the second injection event can be seen. Here clearly piston impingement is visible. Furthermore, the spray area is much smaller because of lower injection duration compared to the previous main injection. After the LED was switched off, at 11°CA, first OH-chemiluminescence flame radiation can be detected. After that, the flame propagates from the spark plug region further into the combustion chamber until it reaches the piston surface at 17°CA ATDC.

At 23°CA first soot radiation intensity is visible next to the piston surface. During this, the flame is still propagating towards the combustion chamber walls. At 41°CA the flame (green) reaches the cylinder walls and also the sooting combustion is distinct (red/orange). For the next crank angles the global distributed chemiluminescence signal decreases whereas the soot radiation signal increases locally (c.f. 47°CA). The images display that the soot radiation signal originates from the piston surface, where it shows its strongest intensity. Based on the injection images it is assumed that there is a fuel film on top of the piston, which evaporates very slowly. This causes a long lasting non-premixed flame structure also termed as poolfire [16]. The following images show that during piston movement in the expansion stroke, liquid ligaments get released from the piston surface, which burn above the top of the surface. These non-premixed flames show characteristic structures which seem to be stationary in the middle of the combustion chamber (c.f. 59°CA - 77°CA). Comparing OH-chemiluminescence and soot intensity at the end of the combustion phase, it seems that the premixed combustion (green) is finished earlier than the sooting combustion (red). This may be a hint to higher engine particle exhaust emissions, since OH*-chemiluminescence can also describe the oxidation process. In addition, the images indicate an asymmetric premixed combustion especially at the end of the combustion stroke (e.g. 71°CA). The flame mainly burns in the left part of the cylinder. This may be caused by lean fuel-air mixtures on the inlet side of the combustion chamber. It is assumed that the fuel from the second injection event is missing for stoichiometric combustion in the area of the inlet valve because of the liquid fuel film. In order to analyze this in more detail and to exclude cyclic variations, the averaged images are used for further consideration.

In Figure 3 (left) the averaged OH-chemiluminescence intensity of the investigated catalyst heating operating point for isooctane, E20, E85 and pure ethanol is displayed. Here the pixel intensities are summed up over 60 averaged image series.

Ethanol shows strongest OH-chemiluminescence intensities and the earliest start of combustion. Considering the position of the maximum intensity the peak appears earliest for E85 and ethanol. It seems that with decreasing ethanol content the start of combustion is retarded. This effect is also visible in the faster initial flame propagation of ethanol which was also reported in [17]. This can be attributed to the higher laminar flame velocity of ethanol in comparison to isooctane [18]. Also the combustion duration is longer for fuels with high isooctane content. It is Remarkable that the absolute chemiluminescence intensity of E20 exceeds those of isooctane and E85. This effect needs further investigation. Considering the 2D-intensity distribution of OH-chemiluminescence, Figure 3 (right) shows averaged images at 36°CA ATDC for all investigated fuels. The time point corresponds to the vertical line in Figure 3 (left). The local intensity distribution is of special interest: For low ethanol contents, the OH-chemiluminescence is inhomogeneous. Especially isooctane and E20 show strong local intensity distributions at the outlet side of the cylinder. Lowest intensity levels can be found in the middle of the image, close to the piston surface. Here the diffusion flame of the poolfire is supposed to suppress the OH-chemiluminescence of the premixed combustion. With increasing ethanol content the combustion becomes more homogeneous. In addition to that, the high chemiluminescence signal of ethanol points out that the mixing process may be much more effective due to the longer injection time and therefore induced charge motion.

In Figure 4 (left) the averaged soot radiation intensity of the investigated catalyst heating operating point for isooctane, E20, E85 and pure ethanol is displayed. On the right hand side the corresponding averaged images are presented for 36°CA ATDC. E85 shows the lowest maximum soot radiation intensity followed by ethanol. Isooctane and E20 show the highest intensity, respectively. After 50°CA ATDC it can be seen that for ethanol and E85 soot radiation is already extinguished. In contrast isooctane and E20 soot radiation lasts long during the cycle. The signal can still be detected at the end of measuring range (at 90°CA ATDC). This time displaced signal is typical for a long lasting poolfire [16]. Comparing Figure 3 (left) and Figure 4 (left) the main combustion zone represented by the OH-chemiluminescence signal decreases earlier as the soot radiation signal for isooctane and E20. It is assumed that with decreased OH-chemiluminescence and increased soot radiation rate the soot oxidation is reduced which can lead to high exhaust particle emission.

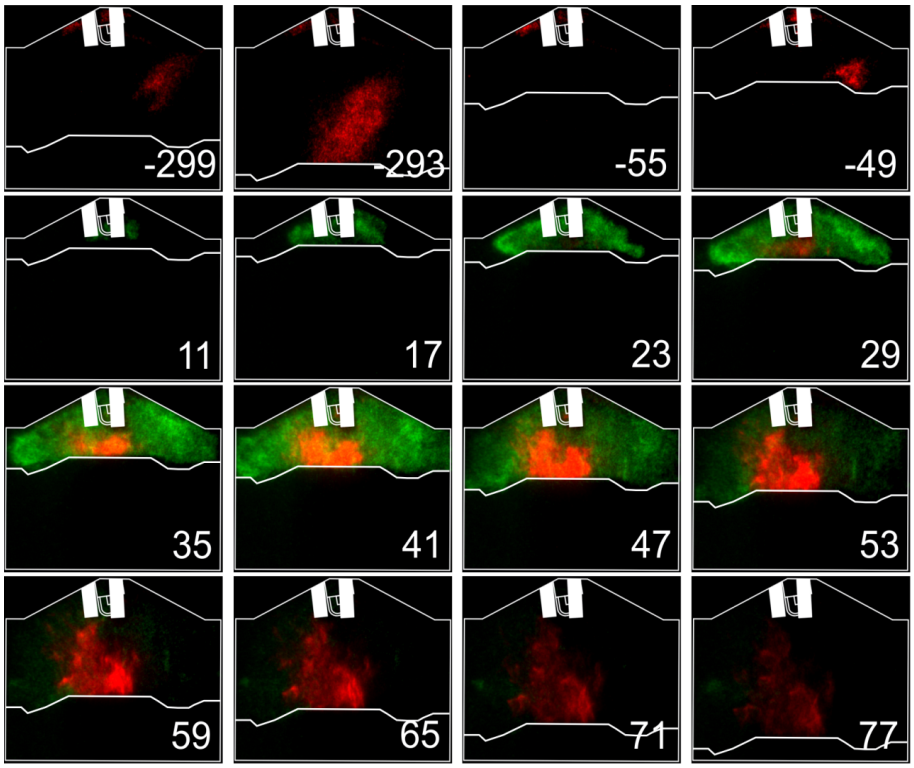

Figure 2. Selected high-speed resolved combustion cycle with double-injection event for isooctane in °CA ATDC. The two wavelength channels "green" for OH-chemiluminescence and "red" for soot luminosity are displayed in one image. Overlapping of these two colors creates "orange" pixel intensities.

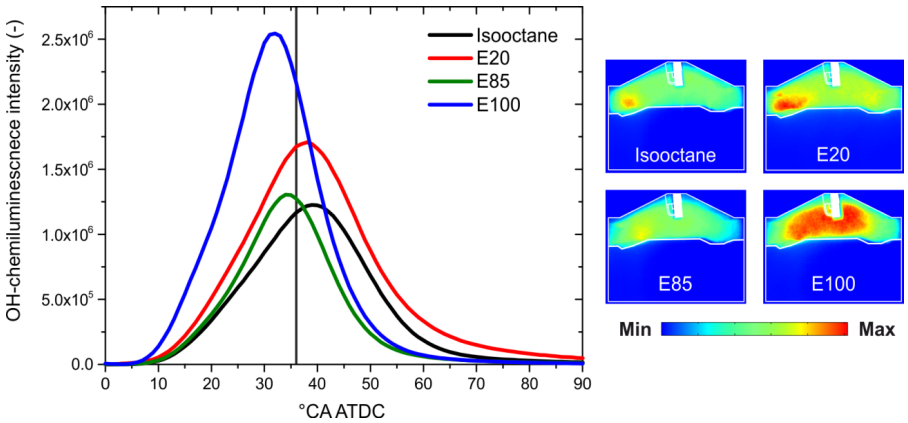

Figure 3. Left: Averaged OH-chemiluminescence intensity of the investigated operating point for isooctane, E20, E85 and pure ethanol. Right: Exemplary averaged images at 36°CA ATDC.

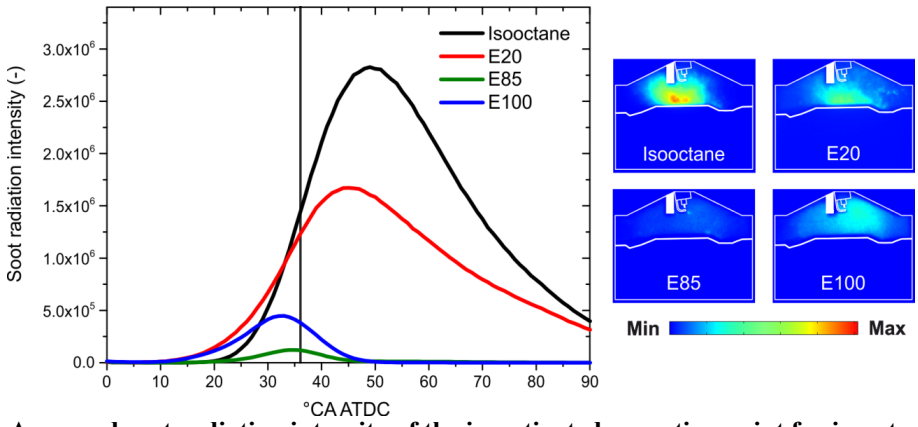

Figure 4. Left: Averaged soot radiation intensity of the investigated operating point for isooctane, E20, E85 and pure ethanol. Right: Exemplary averaged images at 36°CA ATDC.

The decrease of soot radiation intensity with increasing ethanol content indicates that the chemical soot formation mechanisms (fuel oxygen content and carbon chain length) govern the sooting tendency of ethanol blended fuels under these conditions.

Figure 4 (right) shows the spatial distribution of the sooting combustion for the four investigated fuels at 36°CA ATDC (vertical line in Figure 4). Isooctane shows the strongest and most distinct poolfire in middle of the combustion chamber. For E20 the transition between the poolfire and the image background radiation is smoother. Some combustion inhomogeneities can be identified near the piston surface and spark plug for E85 surrounded by background radiation. For ethanol the radiation signal is much stronger than for E85. In addition, the sooting combustion is most homogeneous compared to the other fuels. Here, no poolfire structure can be distinguished although the injected and impinged mass is higher for Ethanol. This may indicate a more effective mixing process for ethanol blended fuels. Especially for ethanol the physical fuel properties (e.g. enthalpy of evaporation) govern the fuel evaporation process [3] at high pressures. These properties could also have a positive impact on the combustion process. Here it is assumed that for a delayed evaporation the fuel momentum and air entrainment is much higher, which can enhance the air and fuel mixing process. Further investigations are necessary in order to clarify this in detail. Since the chemiluminescence signal is much stronger for ethanol and the location of the soot radiation signal meets the location of the OH-chemiluminescence signal, it is assumed that the soot radiation signal does not only originate from soot particles. Here CO-O* broadband continuum could be superimposed in this wavelength region. Since CO-O* broadband radiation also correlates with heat release rate, this could be the source for the higher signal in the wavelength region around 568 nm [19]. However, a detailed spectral analysis of different fuels would reveal further insight into this problem.

The temporal and spatial separation of the two channel combustion radiation already indicates high soot formation rates for E20 and isooctane. In Figure 5 the exhaust particle concentration is quantified for the studied catalyst heating operating point and all investigated fuels. Here the LII-soot sensor was operated for 90 s during the firing period of the optical engine. For this measurement period the results were averaged.

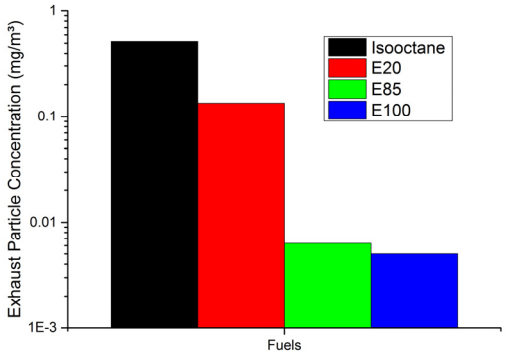

Figure 5. Exhaust particle concentration in mg/m³ measured by LII for the catalyst heating operating point and all investigated fuels.

The exhaust particle concentration correlates with ethanol content. Fuels containing little ethanol show higher particle emissions. For this operation point the chemical soot formation mechanism seems to govern the soot formation of different fuels. This is in good agreement with the high-speed visualization study.

Conclusions

In the present work simultaneous high-speed imaging of OH*-chemiluminescence and natural soot luminosity was performed in an optical accessible engine. For exhaust particle emission correlation a laser-induced incandescence (LII) particle concentration measurement system was applied in the engine exhaust. The effect of ethanol blending on sooting conditions was investigated for isooctane, E20, E85 and pure ethanol. Here, a catalyst heating operating point with strong piston wetting and consecutive poolfire was chosen. Statements about premixed and sooting combustion as well as soot oxidation processes can be made. The main findings can be summarized as follows:

- The high-speed visualization of premixed and sooting combustion offers a robust, qualitative measurement technique in order to evaluate general trends and tendencies in engine combustion. Also particle soot concentrations in the engine exhaust show good correlation with the high-speed imaging measurements.

- With increasing ethanol content the soot formation as well as exhaust emission could be reduced. This reduction can be mainly attributed to different chemical fuel properties which govern the soot formation.

- Both the temporal and the spatial separation of OH*-chemiluminescence and soot radiation intensity indicate increased soot formation rates for isooctane and E20. On the one hand the piston impingement leads to local air-fuel ratio inhomogeneities with rich combustion zones. On the other hand the particles formed by the long lasting poolfire cannot fully be oxidized.

- Although the injected fuel mass and piston impingement is larger for ethanol blended fuels, the combustion is more homogeneous. Here the mixing process may be more efficient, which could be driven by physical fuel properties and increased air entrainment during the longer injection process.

In order to quantify the physical and chemical mechanisms in engine combustion process chain further investigations are necessary. For future work high-speed resolved spectral emission analysis as well as planar laser-induced fluorescence (LIF) measurements of the mixture formation process are planned.

References

[1] W. Piock, G. Hoffmann, A. Berndorfer, P. Salemi, B. Fusshoeller, SAE International Journal of Engines 4 (2011) 1455–1468.

[2] Bronkhorst High-Tech B.V., FLUIDAT pageview 18/11/2014.

[3] T. Knorsch, M. Heldmann, L. Zigan, M. Wensing, A. Leipertz, Exp Fluids 54 (2013).

[4] J. Trost, L. Zigan, A. Leipertz, Proc. Combust. Inst. 34 (2013) 3645–3652.

[5] L. Chen, R. Stone, Energy Fuels 25 (2011) 1254–1259.

[6] M. Salamanca, M. Sirignano, A. D'Anna, Energy Fuels 26 (2012) 6144–6152.

[7] C. S. McEnally, L. D. Pfefferle, Environ. Sci. Technol. 45 (2011) 2498–2503.

[8] P. Price, B. Twiney, R. Stone, K. Kar, H. Walmsley, SAE Technical Paper (2007).

[9] J. P. Szybist, A. D. Youngquist, T. L. Barone, J. M. Storey, W. R. Moore, M. Foster, K. Confer, Energy Fuels (2011) 4977–4985.

[10] L. Chen, R. Stone, D. Richardson, Fuel 96 (2012) 120–130.

[11] M. Storch, L. Zigan, M. Wensing, S. Will, SAE Technical Paper 2014-01-2617 (2014).

[12] E. Stevens, R. R. Steeper, SAE Technical Paper 2001-01-1203 (2001).

[13] A. G. Gaydon, The Spectroscopy of Flames,Chapman & Hall Ltd., London, 1957.

[14] L. C. Haber, U. Vandsburger, Combustion Science and Technology 175 (2003) 1859–1891.

[15] S. Schraml, H. Kremer, R. Sommer, A. Leipertz, COMODIA 2004 (2004).

[16] M. C. Drake, T. D. Fansler, A. S. Solomon, G. A. Szekely, SAE Technical Paper (2003).

[17] P. Sementa, B. Maria Vaglieco, F. Catapano, Fuel 96 (2012) 204–219.

[18] T. Knorsch, A. Zackel, D. Mamaikin, L. Zigan, M. Wensing, Energy Fuels 28 (2014) 1446–1452.

[19] B. Kim, M. Kaneko, Y. Ikeda, T. Nakajima, Proc. Combus. Inst. 29 (2002) 671–677.

Acknowledgement

The authors gratefully acknowledge the financial support by the German Federal Ministry of Food and Agriculture (BMEL) through the Agency for Renewable Resources (FNR), FKZ: 22026711. We also like to thank our project partners Prof. Christian Hasse (NTFD), Prof. Dimosthenis Trimis (GWA, now at Engler-Bunte-Institute Division of Combustion Technology of Karlsruhe Institute of Technology (KIT)) and Prof. Sven Kureti (RT) at TU Bergakademie Freiberg. Furthermore, we acknowledge funding of the Erlangen Graduate School in Advanced Optical Technologies (SAOT) by the German Research Foundation (DFG) in the framework of the German excellence initiative.